AAPS PharmSciTech, Vol. 10, No. 4, December 2009 (© 2009)
DOI: 10.1208/s12249-009-9331-1

Research Article

Novel/Conceptual Floating Pulsatile System Using High Internal Phase Emulsion Based Porous Material Intended for Chronotherapy

Praveen Sher,[1,2,4] Ganesh Ingavle,[2] Surendra Ponrathnam,[2] James R. Benson,[3,4] Nai-Hong Li,[3] and Atmaram P. Pawar[1,4]

Received 7 July 2009; accepted 13 October 2009; published online 20 November 2009

Abstract. The aim of the present study was to design a novel/conceptual delivery system using ibuprofen, anticipated for chronotherapy in arthritis with porous material to overcome the formulation limits (multiple steps, polymers, excipients) and to optimize drug loading for a desired release profile suitable for *in vitro* investigations. The objective of this delivery system lies in the availability of maximum drug amount for absorption in the wee hours as recommended. Drug loading using 3^2 factorial design on porous carrier, synthesized by high internal phase emulsion technique using styrene and divinylbenzene, was done via solvent evaporation using methanol and dichloromethane. The system was evaluated *in vitro* for drug loading, encapsulation efficiency, and surface characterization by scanning electron, atomic force microscopy, and customized drug release study. This study examined critical parameters such as solvent volume, drug amount, and solvent polarity on investigations related to drug adsorption and release mostly favoring low-polarity solvent dichloromethane. Overall release in all batches ranged 0.98–52% in acidic medium and 71–94% in basic medium. These results exhibit uniqueness in achieving the least drug release of 0.98%, an ideal one, without using any release modifiers, making it distinct from other approaches/technologies for time and controlled release and for chronotherapy.

KEY WORDS: chronotherapy; floating pulsatile drug delivery system; high internal phase emulsion; ibuprofen; multiparticulate porous carriers.

INTRODUCTION

In recent years, the quest for understanding the relationship between the performances of a delivery system with regard to internal functioning of human body presents a new therapy regime termed as chronotherapy. Based on circadian rhythm, an internal body clock, which influences various physiological parameters and pathological conditions, points towards time specificity by delivering higher amounts of drug instantly to achieve maximum drug effect. This concept acts contrary to present-day delivery systems based on uniform release (1–8). Various diseases like asthma, hypertension, and arthritis show circadian variation that demand time-scheduled drug release for effective drug action, for example, inflammations associated with morning body stiffness, asthma, and heart attack in the early hours of the day. To follow this principle, an "ideal" dosage form ought to be taken at the convenient time before sleep, providing maximum drug release in the morning (9–13). Various approaches like pulsatile release (14–19) displaying rapid as well as transit release and specific technologies like OROS®, CONTIN®, CEFORM®, TIMERx®, etc. based on various principles and mechanisms have been developed for chronotherapy (20). The major disadvantage of these systems reclines in achieving long residence time which is desired for diseases needing morning medication. To overcome this, novel/conceptual approach termed as "floating pulsatile drug delivery system" was developed (10–13). The basic features of this delivery system comprise of (a) combination of gastroretentive and pulsatile principles, (b) an idealistic drug release profile delivering higher amounts of drug at morning time, (c) low drug release in stomach suited for nonsteroidal anti-inflammatory drug (NSAID) class of drug (ibuprofen, IBU), and (d) multiparticulate systems.

Formulation and development of such and other systems use multiple techniques utilizing high-end machines and multiple-step processes containing different polymers and excipients. These bring with them difficulties like handling equipments and coating core particles for drug release modulation, thereby, generating process variables which become a source of concern (21). To overcome this, porous materials having characteristic and tunable structural properties were used as drug carrier (21–30). Inception of porous material in the development of floating pulsatile drug delivery system (10) associate major significance by behaving as (a) multiparticulate system (b), ensuring the retention of dosage form in the stomach for an extended period without using any other favorable excipients enhancing floating, (c) simulta-

[1] Department of Pharmaceutics, Bharati Vidyapeeth University, Poona College of Pharmacy and Research Centre, Erandwane, Pune, 411038 Maharashtra, India.
[2] Polymer Science and Engineering Division, National Chemical Laboratory, Pune, 411008 India.
[3] Polygenetics, Inc., P.O. Box 33115, Los Gatos, California 95031 USA.
[4] To whom correspondence should be addressed. (e-mail: p_atmaram@rediffmail.com; j-benson@polygenetics.com; sherpraveen@gmail.com)

neous least release all through this period resembling lag phase suited for NSAID drugs to avoid gastric irritation followed by burst release initiated by transit, (d) limit/overcome various formulation variables by acting as a drug loading core using single formulation step when compared with other approaches/methods which need multiple steps.

Earlier application of this concept was performed by using preformed porous polypropylene-based Accurel MP 1000 ®. Overall, the results from various batches using both melt and solvent evaporation to adsorb IBU observed a minimum drug release of nearly 9% in acidic medium set for gastroretentive studies (10,11). However, at the present time, little is known about the *in vivo* performances of the floating pulsatile release system. More knowledge on the *in vivo* investigation of the system should be useful to devices, based on these technologies becoming clinically available (9). Nevertheless, these results prompted the need to study/explore/modify further opportunities by using different porous material for achieving better *in vitro* results and simultaneously understanding various mechanisms.

Another porous material based on the modified synthesis approach of suspension polymerization by high internal phase emulsion (HIPE) technique using styrene and divinylbenzene was explored. Briefly HIPE process is done by combining organic monomers and aqueous discontinuous phases followed by the addition of aqueous suspension medium. On characterization, they are low-density hydrophobic porous material having high surface area with increased connectivity (31). This material, used as "drug carrier," characterizes zero-order release over long periods for a variety of drugs reported previously (32–34).

The objective of the present work was to develop and evaluate a floating pulsatile system by inducing drug adsorption via solvent evaporation, owing to its simplicity, on the porous material synthesized by HIPE technique. Optimization of drug loading and subsequent drug release was done by employing 3^2 factorial design with solvent volume ($X1$) and drug amount ($X2$) as selected variables. IBU, categorized as NSAID, was selected as model drug used in the treatment of arthritis showing circadian variation (9–13). Methanol and dichloromethane, with different polarities, were selected as solvents. Free and drug-loaded microparticles were characterized for practical yield, drug content, crystallinity by differential scanning calorimetry (DSC) and powder X-ray diffraction (XRD), interaction by Fourier transform infrared (FTIR), surface morphology by scanning electron microscopy (SEM) and atomic force microscopy (AFM), extent of decomposition by thermogravimetric analysis (TGA), and porosity by N_2 adsorption. Modified *in vitro* drug release profiling was done by selecting 6 h as the maximum gastric floating time followed by 2 h in basic medium to evaluate the concept of intended drug delivery system (10,11).

MATERIAL AND METHODS

The process for the synthesis of porous copolymer material made of styrene and divinylbenzene by HIPE technique was as described earlier (31). Presently marketed under the trade name of Cavilink™ (from this point onwards, we will refer to the same), they are characterized by hydrophobic nature having a density (typical) of 0.05 to 0.2 g/cm3, internal void volume of 70% to 90%, cavity diameter range of 1 to 50 μm, interconnect pore diameter variable, from small pores to a maximum of 20% of cavity diameter, and surface area of 2–30 m^2/g (32–34).

Materials

IBU was a generous gift from Cipla (India). Methanol (M), dichloromethane (DCM), and other reagents were of analytical grade.

Preparation of Drug-Loaded Beads

Drug Loading

IBU was loaded onto the porous beads by solvent evaporation. The same particle size range was used to nullify the effect of particle size variation. In a typical study, a particular amount of drug was dissolved in selected volume of chosen solvent, followed by the addition of 20 mg of Cavilink. Solvent was further evaporated under ambient conditions overnight.

Factorial Design

Response surface designs allow us to understand the relationship between the various selected variables in experimental area. The experiment based on 3^2 design consisted of nine batches expressed in coded values, Table I, and was used by selecting volume of solvent (X_1) and the amount of drug (X_2) at three different levels. The key factors selected during the optimization were yield, adsorbed drug, drug release at 1, 6, and 7 h, and burst release. All the values were subjected to multiple-regression analysis using statistical software UNISTAT® (statistic version 3, Meglon US) to ensure any interaction.

The equation fitted for this experiment was

$$Y = \beta_0 + \beta_1 X_1 + \beta_2 X_2 + \beta_{11} X_1^2 + \beta_{22} X_2^2 + \beta_{12} X_1 X_2 \quad (1)$$

Where

Y = measured response
X = levels of factors
β = coefficient computed from the responses of the formulations

Evaluation and Characterization of Microparticles

Yield and Percent Drug Adsorbed

The dried weight of microparticles was recorded as practical yield of the process. The drug-loaded beads were dissolved in methanol kept on ultrasonicator, and drug content was assayed by determining in triplicate the absorption at 221 nm using UV spectrophotometer (Jasco V500, Japan). Percent drug adsorbed was used in place of encapsulation efficiency as the drug was adsorbed on surface.

$$\%\ \text{drug adsorbed} = (\text{Actual drug adsorbed}/\text{Total drug amount taken}) \times 100 \quad (2)$$

Table I. Results of Different Evaluation Parameters for Drug-Loaded Porous Microparticles

Batch	Coded levels *X*1:*X*2	Solvent (ml) (*X*1)	Drug (mg) (*X*2)	Practical yield (%)		Drug adsorbed (%)	
				m	d	m	d
1	−1, −1	1	100	98.06±0.58	98.06±0.58	97.67±0.58	97.67±0.58
2	−1, 0	1	200	98.48±1.53	98.94±0.58	98.33±1.53	98.83±0.58
3	−1, 1	1	300	98.23±4.16	99.17±1.15	98.11±4.16	99.11±0.50
4	0, −1	3	100	97.78±1.53	97.78±0.58	97.33±1.53	97.33±0.58
5	0, 0	3	200	95.76±4.73	98.94±0.58	95.33±4.73	98.83±0.58
6	0, 1	3	300	85.00±8.72	99.27±0.58	84.00±8.72	99.22±0.58
7	1, −1	5	100	86.39±1.53	96.11±0.58	83.67±1.53	95.33±0.58
8	1, 0	5	200	94.70±2.08	99.39±0.58	94.17±2.08	99.33±0.58
9	1, 1	5	300	87.92±5.13	99.17±0.58	87.11±5.13	99.11±0.58

m methanol, *d* DCM

Differential Scanning Calorimetry

Thermograms of drug, *Cavilink*, and drug-loaded microparticles were obtained using a Mettler-Toledo DSC 821[e] (Switzerland) instrument equipped with an intracooler. Instrument was calibrated for DSC temperature and enthalpy using Indium standard. The samples were hermetically sealed in perforated aluminum pans and heated at constant rate of 10°C/min over a temperature range of 25–150°C. The system was purged with nitrogen gas at the rate of 100 mL/min to maintain inert atmosphere.

Powder X-ray Diffraction

X- ray powder diffraction patterns of drug and *Cavilink* beads without and with drug were recorded by using a Philips PW 1729 X-ray diffractometer (Netherlands). Samples were irradiated with monochromatized CuK_α radiation (1.542 Å) and analyzed at 2θ between 2° and 40°. The voltage and current used were 30 kV and 30 mA, respectively. The range and the chart speed were 5×10^{3} CPS and 10 mm/2θ, respectively.

Fourier Transform Infrared Analysis

FTIR measurements of drug, *Cavilink*, and drug-loaded ones were obtained on JASCO FTIR 4000 (Japan). Samples were prepared by mixing with KBr and placing in the sample holder. The spectra were scanned over the wavenumber range of 3,600 to 400 cm^{-1} at the ambient temperature.

Surface Topography

Microphotographs of the beads were observed at various magnification using SEM (Cambridge Stereoscan 120, UK) operated with an acceleration voltage of 10 kV. The beads were mounted on the standard specimen mounting stubs and were coated with a thin layer (20 nm) of gold in sputter coater unit (VG Microtech, UK).

Atomic Force Microscopy

AFM measurements were performed in ambient condition on coated pellets without any further sample preparation. The AFM measurements were performed repeatedly on many different microspheres and on several different areas. Although variations were seen, the images presented were typical of those most frequently observed. All the AFM measurements were done in the contact mode using a

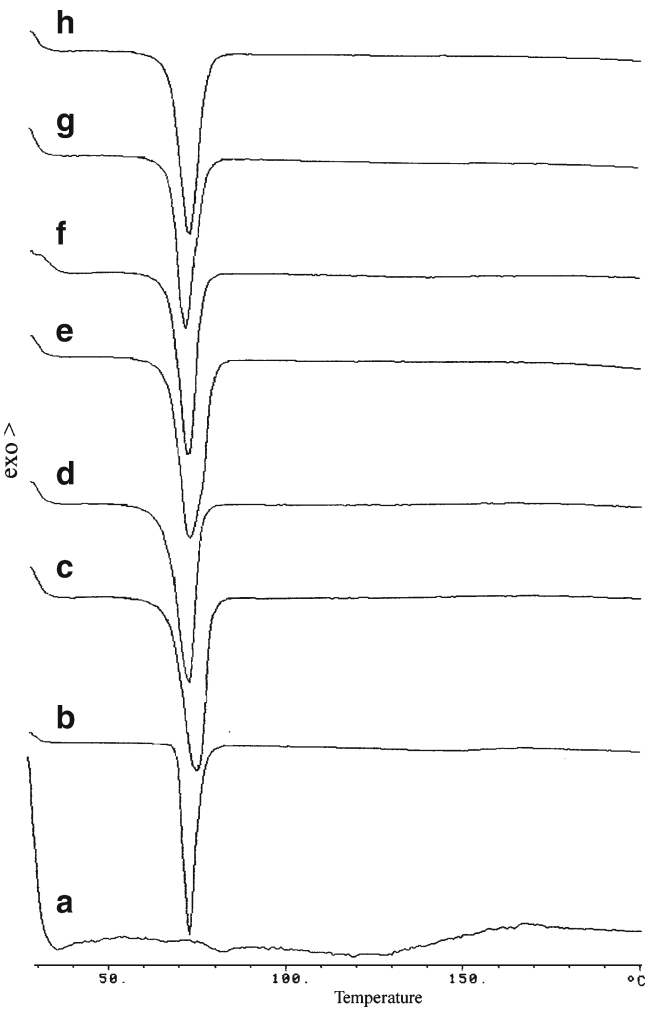

Fig. 1. DSC of (*A*) *Cavilink* ™ microparticles, (*B*) drug, (*C*) batch 1 methanol, (*D*) batch 1 DCM, (*E*) batch 5 methanol, (*F*) batch 5 DCM, (*G*) batch 9 methanol, and (*H*) batch 9 DCM

commercial Multimode with Nanoscope® IV controller (Veeco Instruments Inc., Santa Barbara, CA, USA). Height and deflection images were taken and analyzed using the Nanoscope version 5.12r5 software in the offline mode.

Thermogravimetric Analysis

The drug-loaded microparticles were subjected to gravimetric assay from 35°C to 185°C, with the heat flow of 5°C/min using SEIKO model TG/DTA-32 (Japan). All experiments were performed in the presence of static air.

BET Analysis

Total surface area and the porosity of the *Cavilink* microparticles without and with drug were measured by nitrogen adsorption using a porosimeter (Quantachrome instrument, Autosorb-1™, gas sorption system, ON, Canada). Briefly, weighed amounts of samples were placed in the glass cells and outgassed with nitrogen at 25°C for 3 h before analysis. Subsequently, the sample and the reference cells were immersed in liquid nitrogen at −196°C, and absorption isotherm was obtained from the volume of nitrogen (cm^3/g)

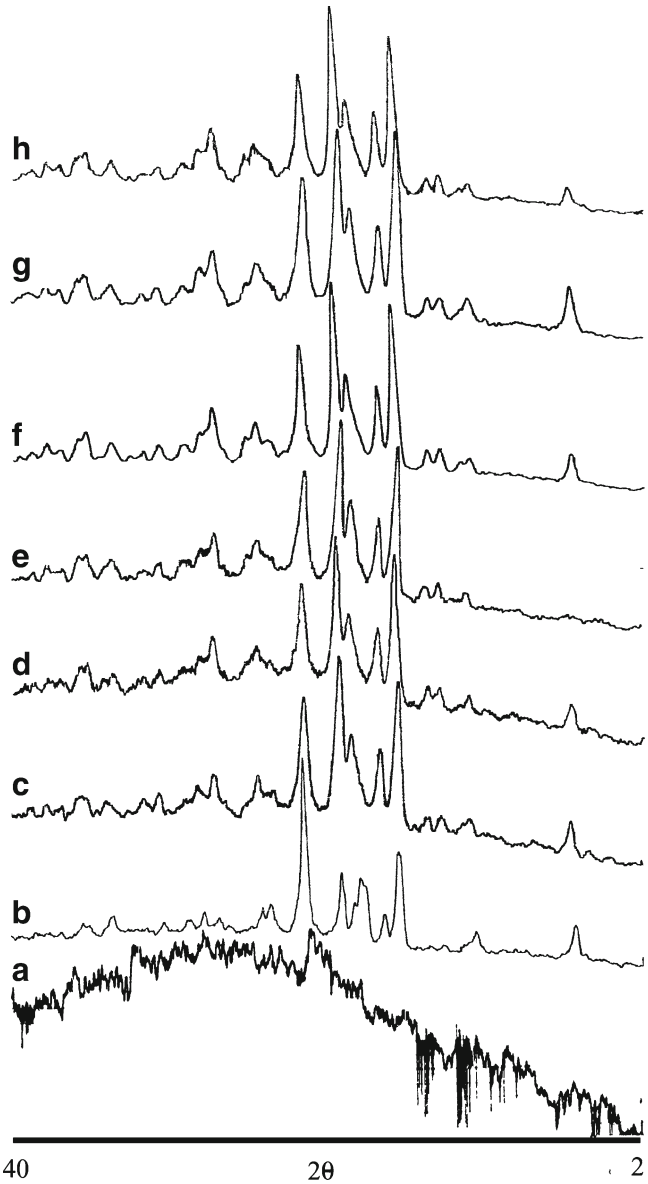

Fig. 2. XRD patterns of (*A*) *Cavilink* ™ microparticles, (*B*) drug, (*C*) batch 1 methanol, (*D*) batch 1 DCM, (*E*) batch 5 methanol, (*F*) batch 5 DCM, (*G*) batch 9 methanol, and (*H*) batch 9 DCM

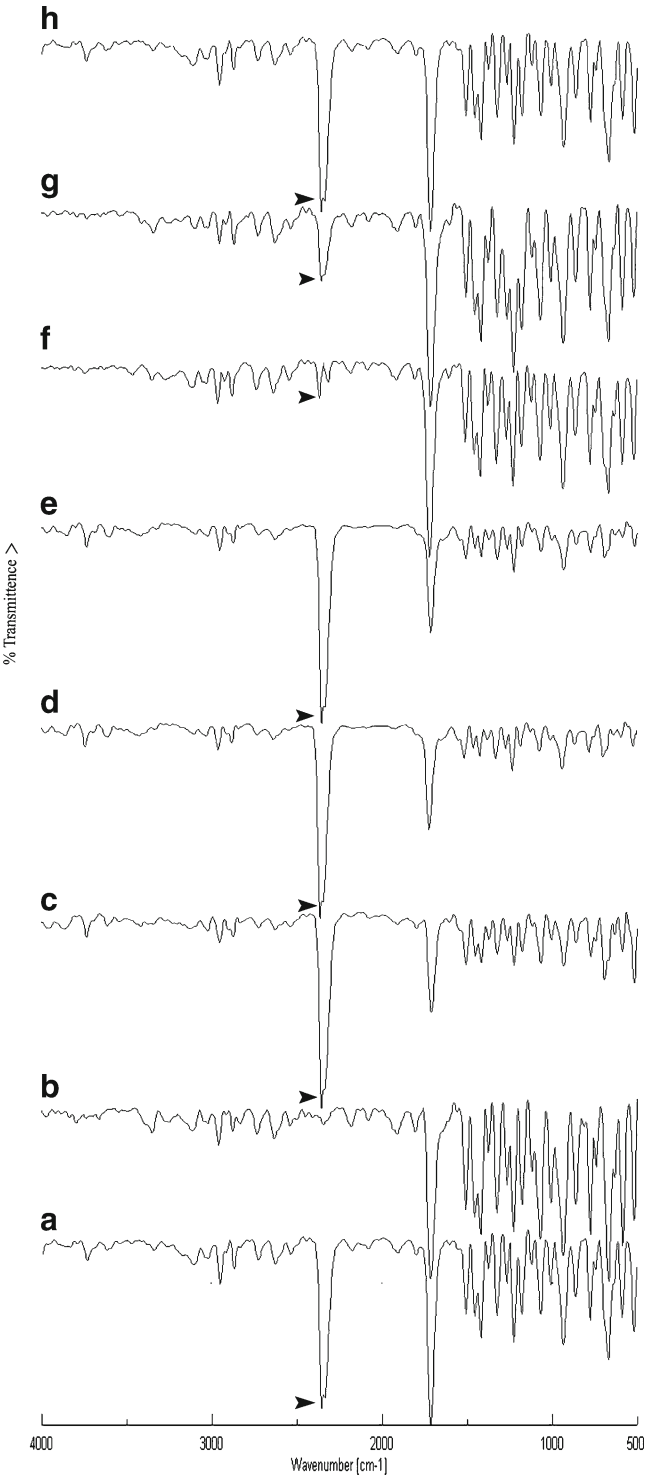

Fig. 3. FTIR spectra of (*A*) *Cavilink* ™ microparticles, (*B*) drug, (*C*) batch 1 methanol, (*D*) batch 1 DCM, (*E*) batch 5 methanol, (*F*) batch 5 DCM, (*G*) batch 9 methanol, and (*H*) batch 9 DCM

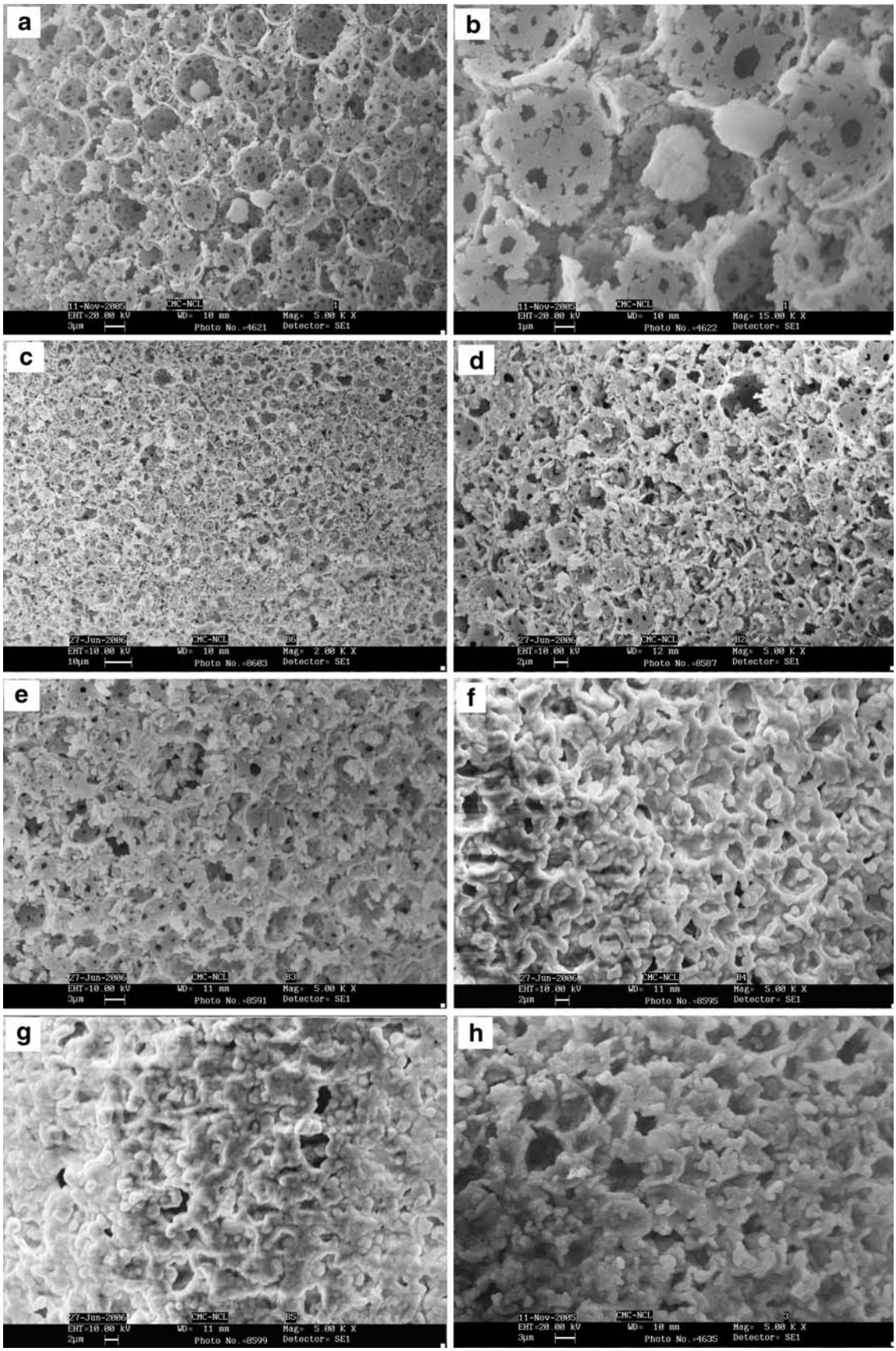

Fig. 4. SEM of **a** batch 1 methanol, **b** batch 1 methanol (higher magnification), **c** batch 3 methanol, **d** batch 9 methanol, **e** batch 5 methanol, **g** batch 1 DCM, **f** batch 5 DCM, and **h** batch 9 DCM

adsorbed onto the surface as a function to relative pressure. Total surface area was calculated by Brunauer–Emmette–Teller (BET) method. Various evaluation parameters were obtained by using Autosorb-1™ software.

In Vitro Dissolution Studies

The dissolution of drug-loaded *Cavilink* beads was studied using USP 26 Type II dissolution test apparatus (Electrolab TDT-06P, India) containing 900 mL of pH 1.2 HCl IP (Indian Pharmacopoeia) and pH 7.2 phosphate buffer IP maintained at 37±0.5°C and stirred at 100 rpm for 6 and 2 h, respectively. Samples were collected periodically and replaced with a fresh dissolution medium. Analysis of data was done using "PCP Disso v2.08" software, India. All the readings were done in triplicate.

Stability Studies

The stability of few selected drug-loaded *Cavilink* batches was monitored up to 3 months at ambient temperature and relative humidity (30°C/60% relative humidity). Samples were removed and characterized by dissolution studies and DSC.

RESULTS

Experiments were designed to adsorb IBU by simple technique of solvent evaporation under ambient conditions onto porous carrier with varying drug amount and solvent volume as shown in Table I. Invariant amount of porous carrier was used in order to minimize/nullify the influence of inherent physical constants (porosity, surface area, or tortuosity) on various interactions during adsorption and release. After preliminary studies, 20 mg of *Cavilink* was selected which was drastically less when compared with 100 mg of Accurel MP 1000 (10,11).

Yield and Drug Adsorbed

Prepared batches were analyzed for yield and drug adsorbed, and results were recorded in Table I. Observed results indicate towards higher minimum values of drug adsorbed using DCM (97%) than using methanol (85%). Decreasing trend was noticed with increasing solvent volume for methanol. This probably can be due to low boiling point, less polar characteristic, and high dielectric constant of DCM along with other pore scale mechanisms leading to high adsorption of drug over the hydrophobic surface (35). Statistical interpretations of the observed values for yield and adsorbed drug amount predict negative influence of solvent volume ($X1$) using methanol for both the responses and positive influence of drug amount in batches prepared using DCM (supplementary data). These results indicate towards preferential drug adsorption interactions influenced by the inherent characteristics of solvent and porous carrier (10,11,30,36)

Evaluation of Drug-Loaded Microparticles

Cavilink, IBU, and IBU-loaded *Cavilink* were evaluated by DSC and XRD to investigate the molecular state of the adsorbed drug molecule in Figs. 1 and 2, respectively. DSC thermograms of the drug-loaded porous polymer and polymer show melting endothermic peaks around 71–74°C, confirming the crystalline nature of the drug even after the adsorption (Fig. 1). Porous carrier, being cross-linked polymers, did not show any melting point. No changes in the nature of either the drug or the polymer after drug loading suggest physical adsorption. This was different from previously reported data suggesting change in the crystalline structure of theophylline adsorbed using solvent evaporation (26). XRD patterns provide supporting evidence for DSC observations corresponding to the retention of the crystalline nature of the drug (Fig. 2). It was observed that characteristics peaks in the region of 1,507 to 2,173 cm^{-1} by FTIR in Fig. 3 showed their presence, indicating dominance of physical interactions. (Main peaks for evaluation are represented by arrowhead.)

Surface Topography

Surface topography in Fig. 4 depicted various patterns of drug adsorption over the porous surface. With methanol, most drug molecules seemed to migrate and attach inside porous network than on the surface (Fig. 4a–e). This can be due to high boiling point leading to slow phase transformation along with hydrophilic (polar solvent)–hydrophobic (surface) interactions. A continuous agglomeration of adsorbed drug confined over the carrier surface was observed using DCM, suggesting no/limited migration of drug into the porous network (Fig. 4f–h). Low boiling point leading to fast phase along with slight hydrophobic (less polar)–hydrophobic (surface) interactions must have led to such an adsorption pattern. Simultaneous evaporation from the hemispherical menisci at each end of the cylindrical pore seems to play a vital role in dictating this type of adsorption pattern (37). Drug adsorption patterns definitely were critical about the characteristics of solvent and surface interactions for drug adsorption.

A contact-mode AFM measurement in air at different magnifications, batch 4 using methanol and DCM, was done for further evaluating the surface morphology (Fig. 5a, b). For batch 4 using methanol, all the corresponding images and 3D plot suggest the true character of the surface. The surface show wavy nature, which is indicated by the light and dark colors in the images, having irregular patterns caused by depressions and counters. Pictures revealed characteristic line arrangements and height conditions of around 1 μm with a nonregular pattern. Lines were easily distinguished as gaps at high magnifications, suggesting the discontinuity of the adsorbed drug layer. This type of surface may be due to various drying phenomena occurring during solvent evaporation; using high polar solvent with hydrophobic surface also seems to show its effect (38). With batch 4 using DCM, Fig. 5c revealed a large concentric area of adsorbed drug with a considerable difference in the layout of adsorbed drug pattern as large compact areas of adsorbed drug with large depth on all sides. On further magnification, the wavy nature becomes more prominent. Figure 5d shows the layered form of adsorption by formation of number of counters with a stepwise formation. No line patterns were observed when compared with the corresponding methanol batch, indicating its continuity over the surface.

TGA study was done to further understand the influence of porous geometry and its relation with drug adsorption profile by studying the melting profile of the drug in Fig. 6. The weight loss pattern follows the same trajectory as that of the drug at the start for batch using DCM but changes later on. This can be due to the presence of the drug at the surface which acts akin to the drug when alone. The shift in the trajectory conjectures the influence of the drug present in pores, which show a shielding effect by limiting the exposure of the drug directly to harsh environmental condition during the experimental process. Batches prepared using methanol show a different trajectory at the start which is contrary to DCM-assisted batch, but the behaviors merge towards the end. These data once again give an insight as well as support the inference about the different drug adsorption patterns discussed above, influenced by the physicochemical behavior of selected variables.

Erratic results were obtained by BET studies. The basic consideration related to this observation indicates the inability of gas adsorption to differentiate modified geometry of drug adsorbed on the surface of porous material. It can be concluded that surface adsorption according to our design of experiment did not seem to comply well with the instrument analysis. A similar type of inference was also projected earlier using porous materials (39).

Drug Release from Porous Carrier

The working of present system resembles the air enclosed system which showed a maximum floating time of 9 h depending upon condition of stomach and supine position of the subject (40). On the basis of subject position (lying during night), working against the principle of floating, study for 6 h was undertaken. *In vitro* dissolution was studied for 6 h in pH 1.2 HCl IP medium (gastroretentive study period), ensuring sink conditions, followed by 2 h in pH 7.2 phosphate buffer IP to mimic increase in pH after transit (10,11). *In vitro* floating was observed visually considering the presence of more than ten to 15 beads below the quarter mark of the dissolution vessel as nonfloating formulations. [In preliminary work, maximum impact of burst release occurred within 10 min followed by very slow release or cutoff using basic medium for the same formulations (data not presented)]. In the present formulation, being a multiparticulate system where no all-at-once emptying is noted, the analysis interval was set at 1 h after changing the medium to normalize anticipated time differences in gastric emptying time and simultaneously the burst effect.

All batches showed varied drug dissolution capacity; the release rate depended on the exposure of the drug, their adsorption pattern, pH, and the modified time frame for the study.

From Methanol Adsorbed Microparticles

The first phase of drug release corresponded to their presence in acidic medium until 6 h, ranging from 1.3% to 52%, followed by the modulated second phase as burst release range from 54.13% to 82.8% to the previous released drug amount after change in dissolution medium. Finally, slow, constant, or no release was observed after burst effect until end release ranged from 71% to 94%. All batches showed excellent *in vitro* floating properties.

Fig. 5. AFM figures of batch 4 using methanol. **a** Deflection and 3D graph at 10 μm; **b** deflection and 3D graph at 4.7 μm, using DCM; **c** deflection and 3D graph at 10.0 μm; **d** deflection and 3D graph at 4.5 μm

Characteristic feature of the observed drug release amount at the end of 6 h decreased with increasing amount of the drug with maximum intradifference using high (5 ml) solvent volume. Synergistic effect of increased surface area effect along with contribution of open pores seizing more dissolution medium at low drug amounts resulted in higher release rates in batches 1, 4, and 7. Drug release difference at different solvent volumes was also observed. Batches using maximum drug amounts for adsorption observed least release irrespective of solvent volume used, indicating akin quantity of drug amount available for mass transfer. Overall difference between the maximum and minimum release at different solvent volumes was nearly 40 times.

Batches 3, 6, and 9 observing release of 1.35%, 1.45%, and 1.30%, respectively, in acidic medium offer a major contribution in the field of time release wherein such low release was achieved without any use of release-retarding polymer or excipient or multiple processes in formulating a delivery system. This also brings in the importance of inherent properties of a typical porous carrier used in this work which can regulate the release profile as observed. Again, this type of release is ideally suited for chronotherapy using IBU by completely reducing the adverse effect caused by of gastric irritation. This release is significantly far less than what we observed previously while using Accurel MP 1000 (9%) (10,11).

Recoded values of drug release at time intervals was preferred over percent release for statistical interpretations at initial (1) and last (6) hour as displayed in Table II. These values predict the negative impact of drug amount coefficient (β) and positive impact of quadratic effect of drug amount factor (β^2). This indicates the interrelationship between porous network and the modifying adsorption patterns contributing to the mass transfer which changes throughout the experiment. Positive solvent effect (α) and solvent volume–drug amount ($\alpha\ \beta$) interaction were observed at initial hour, only signifying the presence of free drug available for dissolution at the start of experiment. The observed values suggest pronounced impact of drug coefficient at all levels irrespective of solvent volume.

Changing to phosphate buffer pH 7.2 IP initiated the sudden increase in release leading to burst release. Maximum burst release fraction was observed in batch 5 at 82.8% (Fig. 7b), favoring middle range of both drug amount and solvent volume. Statistically positive influence of drug and negative influence of drug–drug interaction were observed again, signifying the interaction of different adsorption patterns modified during the dissolution in acidic medium (supplementary results). Comparing with the total drug release at 7 h, the same interaction influences reversed which can be related to synergistic influence of mass transfer in both dissolution mediums.

At the end of experiment, batches 3 and 9 showed slow release, while cutoff was observed in all other batches. This observation can be related to the various interface phenom-

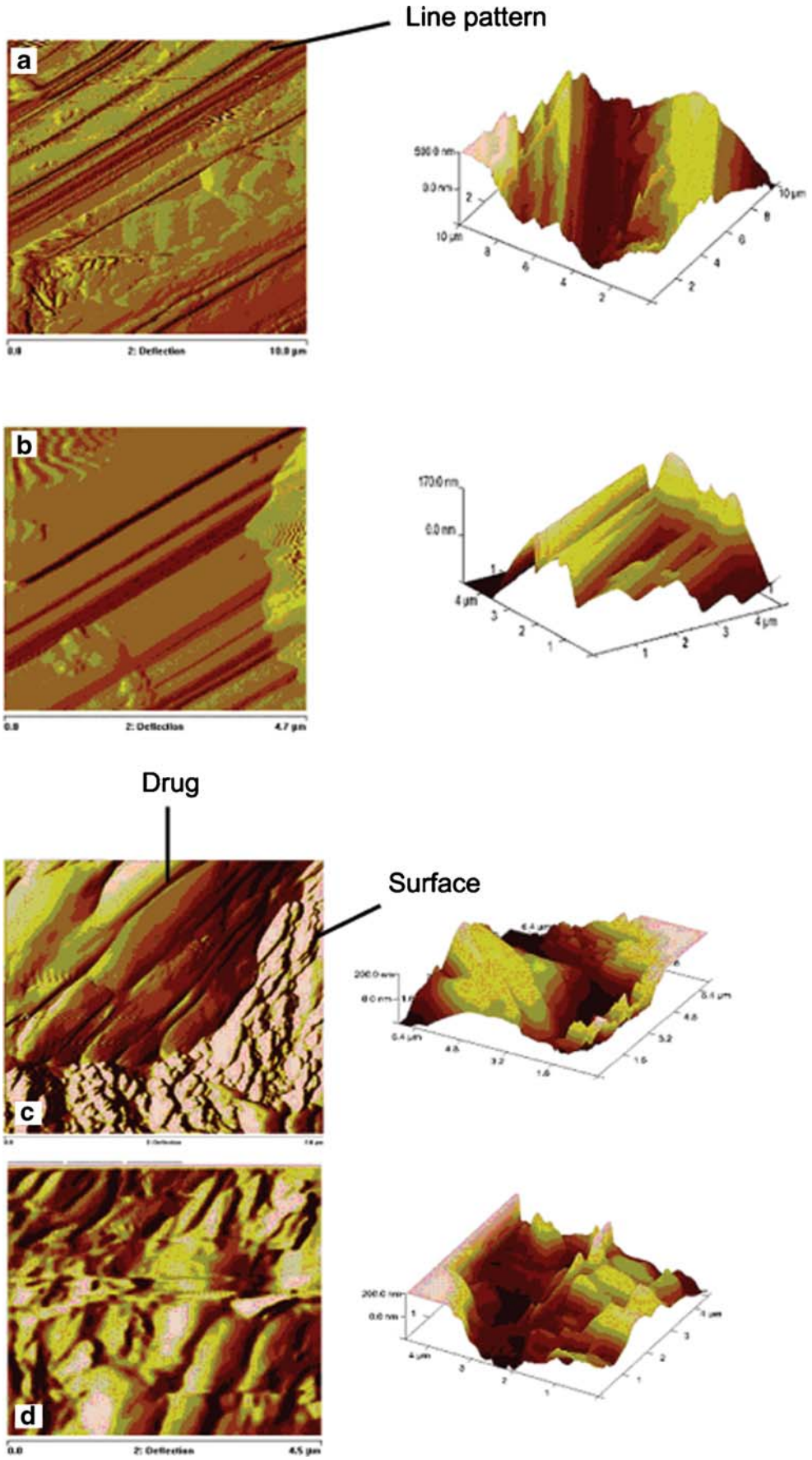
Line pattern
a
b
Drug
Surface
c
d

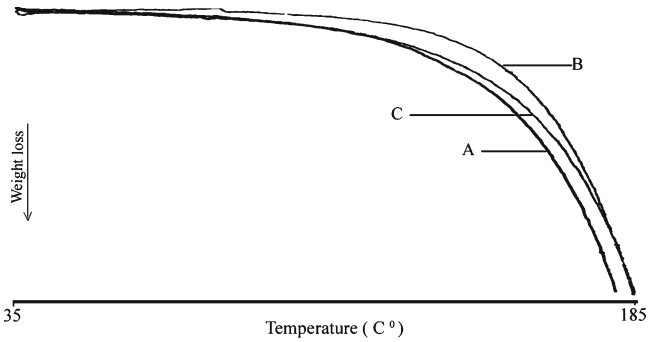

Fig. 6. TGA of (*A*) drug, (*B*) batch 9 methanol, and (*C*) batch 9 DCM

ena which change along with time progression. Batch 5 can be considered as optimized formulation for the purpose of chronotherapy with 1.79% release in acidic medium followed by burst of 82.8%. Also, batch 9 can also be preferred as the subsequent choice with 1.3% release in acidic medium followed by 72.83% burst release (Fig. 8).

From DCM Adsorbed Microparticles

Observed release rates as low as 0.98% to a maximum of 2.84% were recorded in acidic medium. Burst release and final release ranged 71% to 87% and 74% to 89%, respectively (Fig. 9). All batches showed excellent *in vitro* floating properties except for 1, 4, and 7 prepared using the least amount of drug (100 mg), which remained afloat for 3 h only. The exact reason for this is to be yet understood but probably can be due to different drug adsorption patterns influencing buoyancy influenced by mass transfer.

The release in acidic medium showed a characteristic trend recording the least release for batches using high level of drug (300 mg) irrespective of solvent volume used. Various parameters influencing the drug release seem to replicate as observed in methanol batches. The least/less drug release can also be related to the difference in adsorption pattern due to solvent property.

Batch 6 recorded the overall least release of 0.98% without using any excipient or any release modifier, Fig. 9b. Once again, such results vindicate present drug delivery concept and formulation along with application of Cavilink™ in the field of timed drug release.

Statistical assumption could be utilized for the initial hour only as all batches did not have a 6-h floating time. Predictions for initial and third hour readings as recorded in Table II indicate a negative influence of drug amount (β) along with drug–drug (β^2) interaction for the former readings only. The

Table II. Estimation of Regression Coefficients for Different Response Variables

Responses	% Release at 1 h		% Release at 6 h	% Release at 7 h
Coefficient	m	d	m	m
C	0.642	0.883	2.346	77.753
α ($X1$)	0.522	–	–	–
β ($X2$)	−5.32	−0.312	−20.90	−10.33
α^2 ($X1 \cdot X1$)	–	–	-	-
β^2 ($X2 \cdot X2$)	5.06	-0.419	19.92	5.60
$\alpha\,\beta$ ($X1 \cdot X2$)	0.94	–	–	–
R^2	0.9931	0.9179	0.9649	0.8868
Sig.	0.0001	0.0006	0.0000	0.0014

– not in a function

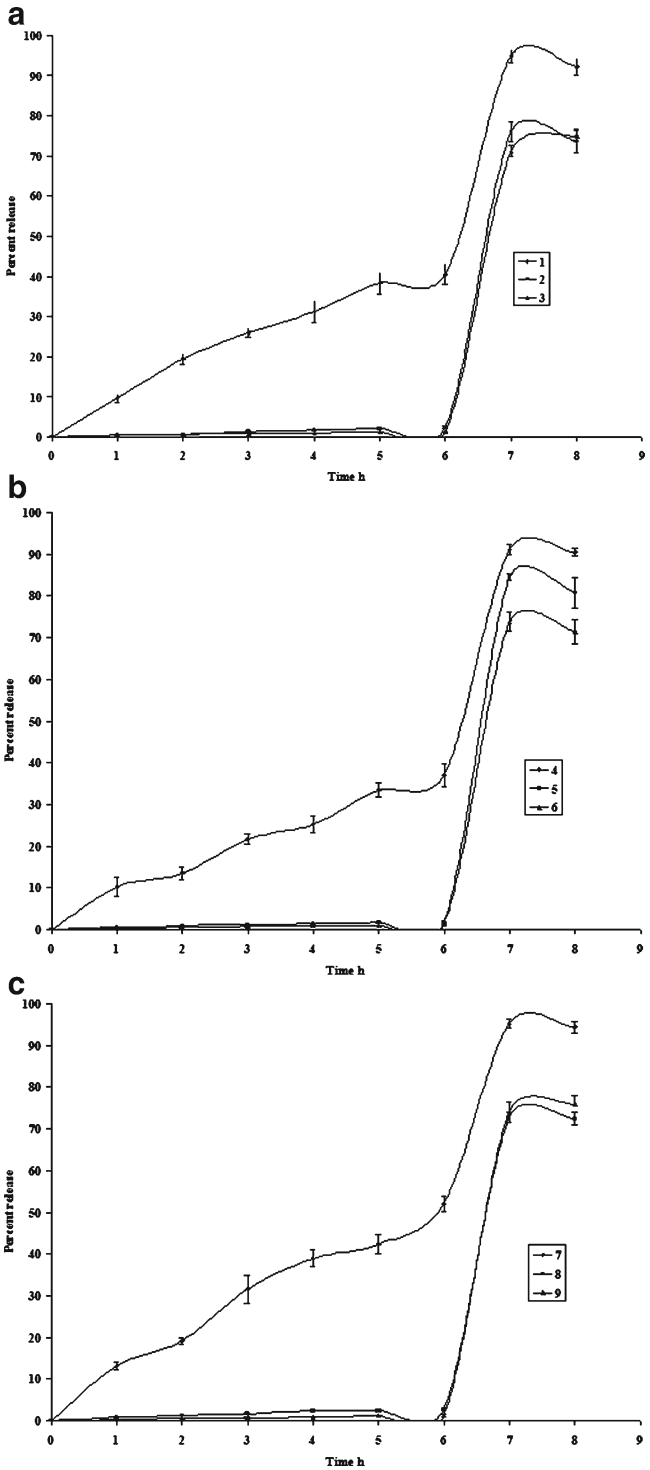

Fig. 7. Cumulative drug release profile using methanol. **a** Drug release using 1 ml, **b** drug release using 3 ml, **c** drug release using 5 ml

response surface graphs (Fig. 10) also vindicate the stand showing change of curvilinear graph to a somewhat straight one.

Changing the medium provided with the same form of drug release profile as was observed akin to batches. Batches 1, 4, and 7 displayed a conventional form of pulsatile delivery system. Statistical analysis was of limited use as all batches did not show the desired floating property.

Overall, batches 2 and 5 look promising for this type of delivery. Batch 5 showed a slight edge due to less release in acidic medium.

Stability studies predict no significant changes in the drug release. Apart from this, DSC and XRD show the same results with marginal difference.

DISCUSSION

In this paper, we studied the adsorption pattern and their influence on the release profile of model drug, IBU, from porous material synthesized by HIPE for formulating an ideal floating pulsatile drug delivery system intended for chronotherapy in arthritis. Drug adsorption by solvent evaporation under ambient conditions was preferred over other methods for its ease and single-step process (16,21,24–27). Herein, adsorption process commences with the contact and penetration of solvent followed by its positioning through the geometric porous network, depending on both molecular and bulk properties of the solvent along with surface property of the porous material (41). Other properties like pore size, pore shape, surface tension of solvent, and contact angle between surface and solvent initiate the requisite disarticulation (36,42,43). Apart from this, it can be also presumed that during solvent evaporation continuous change in volume of the drug-loaded solvent influenced by the boiling point seems to play an important role. Influence of solvent levels changes the impact of capillary gradients present when a porous material is in contact with little solvent volume which disappears at complete solvent saturation/submerging and change to pressure gradients (44). Both conditions work synergistically or differently depending on the boundary line conditions influencing adsorption and mass transfer. Thus, at increased solvent volume, the aggregation tends to be a little lower, suggesting a shift of adsorbate inside the porous matrix.

At molecular-level interaction, many pore-scale mechanisms such as the motion of individual gas–liquid meniscus residing in the pore spaces, diffusion in gas and liquid phase, capillarity and possible flow through connected films, etc. show their influence (41). All these mechanisms/phenomena must have behaved differently during a slow-phase transition using methanol than DCM leading to different adsorption patterns which in turn affect the yield. Also, the interactive behavior of drug, IBU, having both polar –COOH and a nonpolar CH (CH_3) C_6H_4 CH_2 CH $(CH_3)_2$ groups, display various polar interactions between each other using methanol. The magnitude of this reaction has been found to be dependent upon free energy of solid and the dispersed adsorbate which in the present work would be varying with increasing drug amount and decreasing solvent volume (45). However, the last interactive behavior will be probably less/absent for DCM, being a less polar solvent, displaying a characteristic pattern based on the geometrical/structural representation of individual pore network (37).

All these processes during and after the adsorption process is over give rise to the alteration in a porous skeleton due to drug deposition. The depositions occur at favorable site within the network which displayed marked difference using different polarity solvents. This modification of inner geometry with relation to total porosity gives rise to two definite areas as continuous and discontinuous clusters. As the name suggests, continuous clusters in a pore network are those areas where drug adsorption is connected/concentrated to each other, while discontinuous clusters are the opposite,

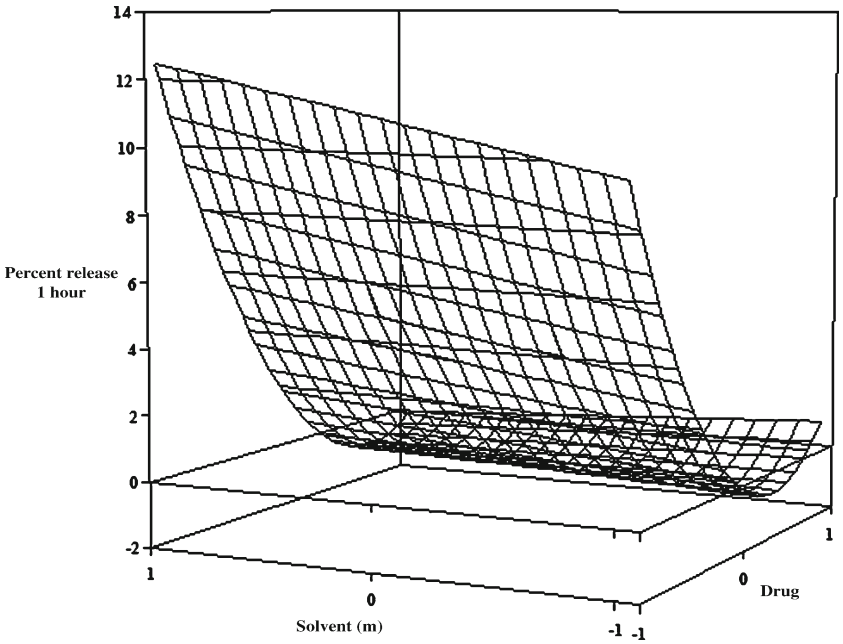

Fig. 8. Response surface plot showing effect of variables on drug release at 1 h using methanol

having isolated adsorption areas with no contact with other drug absorbed area. The deposition pattern showed lots of open, individual acting, areas with crystal drug forms mostly at pore ends using methanol, indicating towards discontinuous clusters. This can be due to solvent nature behavior as suggested above. But for DCM the contrary was observed with large continuous clusters forming at the surface. This can be one reason for having high percentage of drug adsorption (36).

Dissolution in porous media results in the scale removal which most likely occurs at pore surface. Interaction of dissolution medium which starts with filling of pores followed by its diffusion through same towards outside leads to mass transfer from the porous material. Again, here, we have a differentiation which helps in understanding the dissolution and mass transfer process. They are characterized as contributing or effective and noncontributing porosity. As the name suggests, contributing porosity is linked with areas where pore spaces are/appear open, allowing flow through properties. This aspect was quite evident on the surface using methanol. Another feature where the physically isolated pore spaces correspond to hindrance in the flow through properties is referred to noncontributing porosity (36). This was quite evident with DCM-related adsorption pattern. Overall, both these terms can also be referred to single porous system also depending on the characteristic adsorption pattern.

This accounts for a change in pore volume which in turn depended on the deviation of the saturation ratio, volume of pore fluid, and affinity of the pore surface. Saturation ratio depending on the drug solubility in that medium undergoes different phases like undersaturation, equilibrium, and supersaturation based on the positioning of drug in a particular area (36). Gurny *et al.* (46) had given an excellent understanding of the drug release from porous polymers. All these processes take place in real time which keeps on changing depending on impact of all or some of preceding factors pertinent at that moment influencing the concentration distribution dynamics of entrapped/dissolved components. In addition to this, roughness of surface which increases the hydrophobicity as well gives rise to multiple dissolution fronts also plays their role in such systems (47). The increase in hydrophobicity may directly affect the pore volume which in turn influences the mass transfer of component. The flow, nature, and the interaction of dissolution medium inside the porous material may be referred to a rate-limiting step.

All these factors working in tandem may well be the real cause of achieving such low releases without using any release modifiers which are truly significant in the field of time and controlled release. The low release observed might be caused by the least penetration of dissolution medium which must be aggravated by the solubility and also by the increase in the hydrophobicity of the system working together. Low pore volume due the influence of particular adsorption pattern can be a major contributing factor for this type of release. The contrary was true for batches with low drug amount, suggesting the positive influence of above factors in modulating the drug release showing significantly higher releases.

During dissolution, sudden depletion of adsorbed drug clusters serving as reservoirs directing new boundary conditions expose rough and hydrophobic nature of surface and pores to dissolution medium, thereby retarding/stopping the drug release. Influence of noncontributing porosity, where no mass transfer takes place, also leads to cutoff. Segal *et al*. had reported cutoff or recovery for unreleased amount of drug from porous matrices (48). Moving boundary conditions influencing geometry have been earlier discussed by Stephan moving problem (49,50). This influence was perfectly

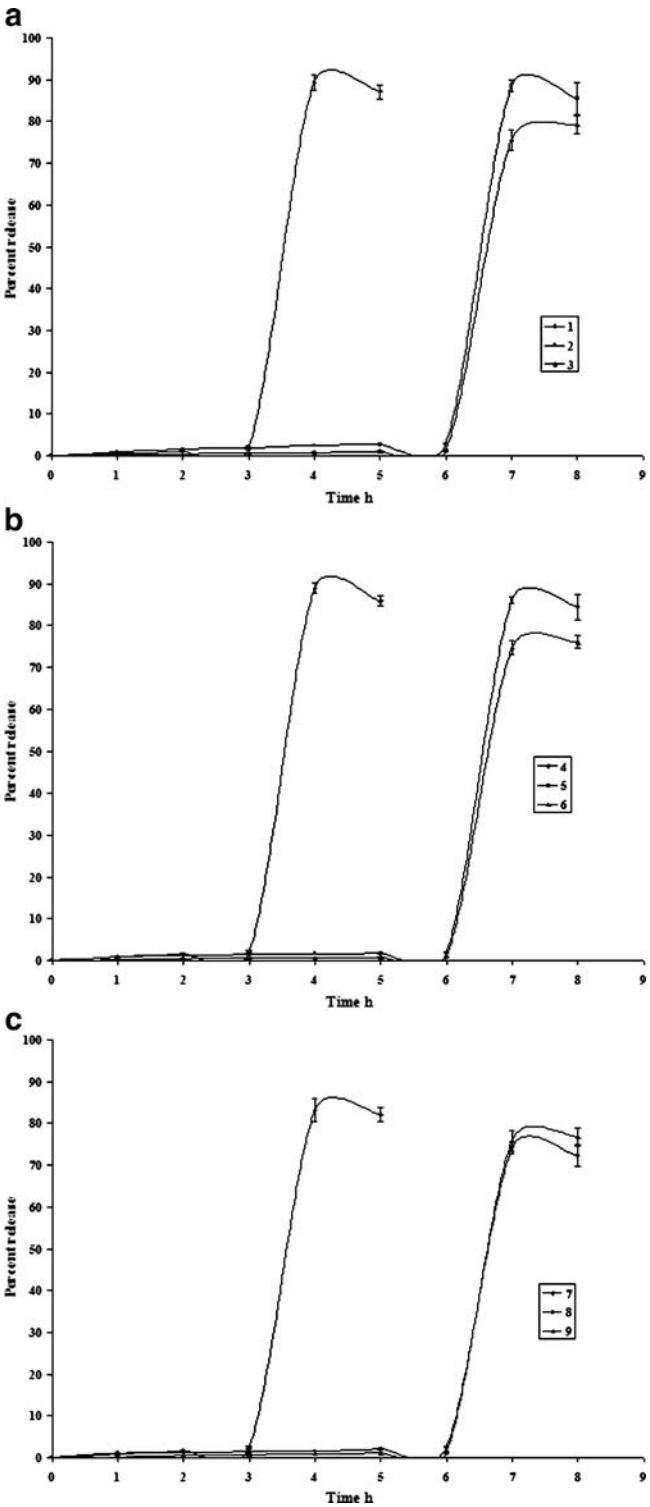

Fig. 9. Cumulative drug release profile using DCM. **a** Drug release using 1 ml, **b** drug release using 3 ml, **c** drug release using 5 ml

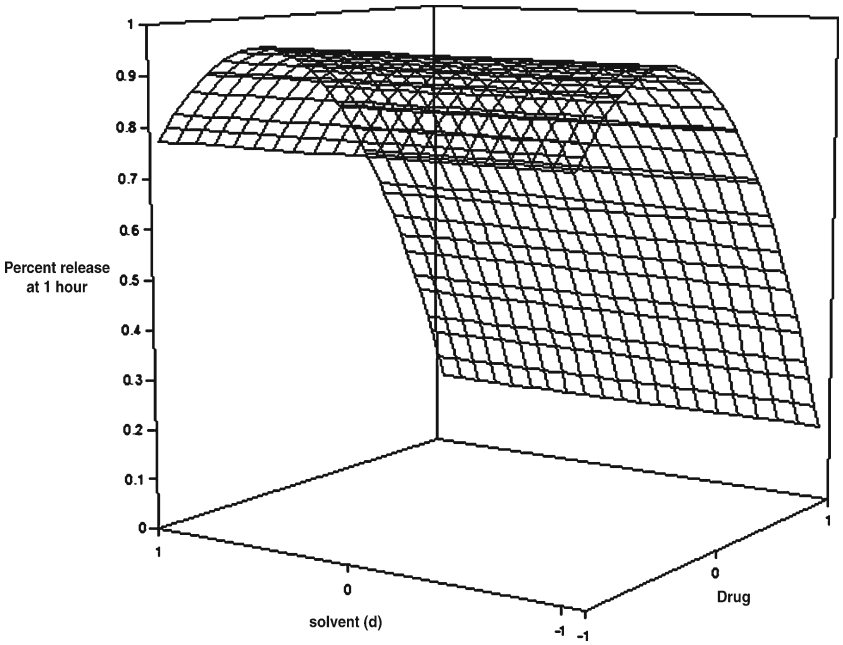

Fig. 10. Response surface plot showing effect of factorial variables on drug release at 1 h using DCM

observed in drug release while exposing porous carriers to basic medium alone than using acidic medium prior to it.

CONCLUSION

In this paper, we envisaged the concept of combining floating and pulsatile principles to meet the requirements of "idealistic" delivery system for chronotherapy purpose intended for arthritis. Termed as floating pulsatile drug delivery system, it merges the programmed and triggering systems, which otherwise behave independently. Floating or gastroretentive action can be related to programmable system using low-density carriers as an ideal choice while triggering mechanism system is influenced by the change in the pH. This form of delivery system can be used for drugs showing pH-dependent solubility or having adsorption window where solubility and adsorption of particular class of drugs increases.

Drug release from porous material has shown distinct variability mostly favoring fast release. This experimental procedure using HIPE-based porous material demonstrates excellent retardation of drug release near the negligible levels without any use of additives which mark their effective implications for the development of the "idealistic" drug delivery system based on "floating pulsatile drug delivery systems," using IBU without any additives. All the processes governing the drug release in both solvent-assisted drug loading have nearly the same influence for mass transfer except that the release quantum which is governed by the adsorption geometry is influenced by their characteristics. Critical balance between continuous and discontinuous clusters during adsorption leading to contributing and noncontributing porosity during dissolution plays important roles in the observed drug release pattern.

ACKNOWLEDGMENTS

Praveen Sher and Atmaram Pawar are thankful to University Grants Commission, India, for providing major research project. Authors are thankful to Dr. Smita Mule (DSC), A.B. Gaikward (SEM), Dr. Pankaj Poddar and Baishakhi (AFM) for help in evaluation.

REFERENCES

1. Smolensky MH, Haus E. Circadian rhythms and clinical medicine with applications to hypertension. Am J Hypertens. 2001;14:280S–90S.
2. Percel PJ, Vyas NH, Vishnupad KS, Venkatesh GM. Pulsatile release histamine H2 antagonist dosage form. US Patent 6663888, 2003.
3. Office of Technology Assessment, United States Congress. Biological rhythms: implication for the worker. US Government Printing Office: Washington DC; 1991. p. 37–66.
4. Smolensky MH. Chronobiology and chronotherapeutics application to cardiovascular medicine. Am J Hypertension. 1996;9:11S–21S.
5. Lemmer B. The clinical relevance of chronopharmacology in therapeutics. Pharmaco Res. 1996;33(2):107–15.
6. Mormont M, Levi F. Cancer chronotherapy: principles, applications, and perspectives. Cancer. 2003;97(1):155–69.
7. Cutolo M, Seriolo B, Craviotto C, Pizzorni C, Sulli A. Circadian rhythms in RA. Ann Rheum Dis. 2003;62:593–6.
8. Stubbe BG, Smedt S, Demeester CD. Programmed polymeric devices for pulsed drug delivery. Pharma Res. 2004;21(10):1732–40.
9. Zou H, Jiang X, Kong L, Gao S. Design and evaluation of a dry coated drug delivery system with floating-pulsatile release. J Pharm Sci. 2008;97:263–73.
10. Sher P, Ingavle G, Ponrathnam S, Pawar AP. Low density porous material based conceptual drug delivery system. Micro Meso Mater. 2007;102:290–8.
11. Sher P, Ingavle G, Ponrathnam S, Poddar P, Pawar AP. Modulation and optimization of drug release from uncoated

low density porous carrier based delivery system. AAPS PharmSciTech. 2009;10:547–58. doi:10.1208/s12249-009-9239-9.
12. Badve SS, Sher P, Korde A, Pawar AP. Development of hollow/porous calcium pectinate beads for floating pulsatile drug delivery. Eur J Pharm Biopharm. 2007;65:85.
13. Sharma S, Pawar A. Low density multiparticulate system for pulsatile release of meloxicam. Int J Pharm. 2006;313:150–8.
14. Dashevsky A, Mohamad A. Development of pulsatile multiparticulate drug delivery system coated with aqueous dispersion Aquacoat® ECD. Int J Pharm. 2006;318:124–31.
15. Efentakis M, Koligliati S, Vlachou M. Design and evaluation of a dry coated drug delivery system with an impermeable cup, swellable top layer and pulsatile release. Int J Pharm. 2006;311:147–56.
16. Li Y-H, Zhu J-B. Modulation of combined-release behaviors from a novel "tablets-in-capsule system". J Cont Release. 2004;95:381–9.
17. Lee B-J, Ryu S-G, Cui J-H. Controlled release of dual drug-loaded hydroxypropyl methylcellulose matrix tablet using drug-containing polymeric coatings. Int J Pharm. 1999;188:71–80.
18. Lee B-J, Min G-H. Oral controlled release of melatonin using polymer-reinforced and coated alginate beads. Int J Pharm. 1996;144:37–46.
19. Bussemer T, Bodmeier R. Formulation parameters affecting the performance of coated gelatin capsules with pulsatile release profiles. Int J Pharm. 2003;267:59–68.
20. Ravishankar H, Patil P, Samel A, Petereit H-U, Lizio R, Iyer-Chavan J. Modulated release metoprolol succinate formulation based on ionic interactions: *in vivo* proof of concept. J Cont Release. 2006;111:65–72.
21. Ohta KM, Fuji M, Takei T, Chikazawa M. Development of a simple method for the preparation of a silica gel based controlled drug delivery system with a high drug content. Eur J Pharm Sci. 2005;26:87–96.
22. Charnay C, Begu S, Tourney-Petelh C, Nicole L, Lerner DA, Devoisselle JM. Inclusion of ibuprofen in mesoporous templated silica: drug loading and release property. Eur J Pharm Biopharm. 2004;57:533–40.
23. Song SW, Hidajat K, Kawi S. Functionalized SAB-15 material as carrier for controlled drug delivery: influence of surface properties on matrix–drug interactions. Langmuir. 2005;21:9568–75.
24. Gren T, Nystrom C. Porous cellulose matrices containing lipophilic release modifiers—a potential oral extended-release system. Int J Pharm. 1999;184:7–19.
25. Streubel A, Sipemann J, Bodmeier R. Floating microparticles based on low density foam powder. Int J Pharm. 2002;241:279–92.
26. Streubel A, Sipemann J, Bodmeier R. Multiple unit gastroretentive drug delivery systems: a new method for low density microparticles. J Microencapsul. 2003;20(3):329–47.
27. Sharma S, Sher P, Badve S, Pawar AP. Adsorption of meloxicam on porous calcium silicate: characterization and tablet formulation. AAPS PharmSciTech. 2005;6:E618–25.
28. Byrne RS, Deasy PB. Use of commercial porous ceramic particles for sustained drug delivery. Int J Pharm. 2002;246:61–73.
29. Wang C, He C, Tong Z, Liu X, Ren B. Combination of adsorption by porous $CaCO_3$ microparticles and encapsulation by polyelectrolyte multilayer films for sustained drug delivery. Int J Pharm. 2006;308:160–7.
30. Sher P, Ingavle G, Ponrathnam S, Pawar AP. Low density porous carrier: drug adsorption and release study by response surface methodology using different solvents. Int J Pharm. 2007;331:72–83.
31. Li NH, Benson JR, Kitagawa N. Polymeric microbeads and method of preparation. European Patent EP0764047, 2003.
32. Landgraf W, Nai-Hong L, Benson JR. New polymer enables near zero-order release of drugs. Drug Deliv Tech. 2005;5(2):48–55.
33. Landgraf W, Nai-Hong L, Benson JR. Polymer microcarrier exhibiting zero-order release. Drug Deliv Tech. 2003;3(1):56–63.
34. Benson JR. Highly porous polymers. Amer Lab. 2003;35(10):44–52.
35. Gunko VM, Mikhalovskii SV, Melillo M, Voronin EF, Nosach LV, Pakhlov EM. The effect of the nature and structure of adsorbents on interaction with ibuprofen. Theor Exp Chem. 2004;40:3.
36. Civan F. Scale effect on porosity and permeability: kinetics, model and correlation. AIChE J. 2001;47(2):271–87.
37. Sarkisov L, Monson PA. Modeling of adsorption and desorption in pores of simple geometry using molecular dynamics. Langmuir. 2001;17:7600–4.
38. Scott DC. An assessment of reasonable tortuosity values. Pharm Res. 2001;18:1797.
39. Salonen J, Laitinen L, Kaukonen AM, Tuura J, Bjorkqvist M, Heikkila T, *et al*. Mesoporous silicon microparticles for oral drug delivery: loading and release of five model drugs. J Cont Release. 2005;108:362–74.
40. Iannuccelli V, Coppi G, Sansone R, Ferolla G. Air compartment multiple-unit system for prolonged gastric residence. Part II. *in vivo* evaluation. Int J Pharm. 1998;174:55–62.
41. Yiotis AG, Stubos AK, Boudouvis AG, Yortsos YC. A 2-D pore-network model of the drying of single-component liquids in porous media. Adv Water Res. 2001;24:439–60.
42. Rozwadowski M, Lezanska M, Wloch J, Erdmann K, Golembiewski R, Kornatowski J. Mechanism of adsorption of water, benzene, and nitrogen on Al-MCM-41 and effect of coking on the adsorption. Langmuir. 2001;17:2112–9.
43. Horcajada P, Ramila A, Perez-Pariente J, Vallet-Regi M. Influence of pore size of MCM-41 matrices on drug delivery rate. Micro Meso Mater. 2004;68:105–9.
44. Germann PF, DiPietro L. When is porous-media flow preferential? A hydromechanical perspective. Geoderma. 1996;74:l–21.
45. Janczuk B, Chibowski E, Wojcik W. The influence of *n*-alcohols on the wettability of hydrophobic solids. Powder Technol. 1985;45:1–6.
46. Gurny R, Doelker E, Peppas NA. Modeling of sustained release of water-soluble drugs from porous, hydrophobic polymers. Biomaterial. 1982;3:27–32.
47. Chen Y, He B, Lee J, Patankar NA. Anisotropy in the wetting of rough surfaces. J Coll Inter Sci. 2005;281:458–64.
48. Siegel RA, Kost J, Langer R. Mechanist studies of macromolecular drug release from macroporous polymers. I experiments and preliminary theory concerning completeness of drug release. J Cont Release. 1990;8:223–36.
49. Collins R. Mathematical modeling of controlled release from implanted drug-impregnated monoliths. Pharm Sci Tech Today. 1998;1(6):269–76.
50. Collins R, Jinuntuya N, Petpirom P, Wasuwanich S. Mathematical model for controlled diffusional release of dispersed solute drugs from monolithic implants. Biotransport: heat and mass transfer in living systems. Ann N Y Acad Sci. 1998;858:116.